SUPPLEMENTAL DATA

SUPPLEMENTARY FIGURE LEGENDS

Figure 1. Analysis of the LRRK2 dimer.

(**A**) LRRK2 expression varied substantially across cell lines. The levels of LRRK2 were analyzed in lymphoblasts expressing endogenous LRRK2, HEK293FT and MES cells transiently transfected with LRRK2 constructs. Similar amounts of protein were loaded onto the gel as shown by the GAPDH loading control.

(**B**) Expression levels of LRRK2 do not affect its distribution across the glycerol gradient. LRRK2, expressed at a relatively low level in MES cells (Figure S1a), is found in LMW and HMW fractions, almost identical to LRRK2 profile from HEK293FT cells (Figure 1). Western blots from glycerol gradient fractions using whole-cell extracts of dopaminergic MES cells transfected with myc-WT LRRK2. Anti-myc antibody was used to detect transfected LRRK2.

(**C**) A minority of LRRK2 is present as a heterodimer as assessed by heterologous co-IP following co-expression of GFP- and myc-LRRK2 in HEKFT cells. The myc-resin pulls down smaller amounts of GFP-LRRK2 than myc-LRRK2 (*lane 4*), illustrated by the fact that a higher proportion of the same IP is needed to obtain similar band intensity (relative to input). The GFP capture antibody pulls down smaller amounts of myc-LRRK2 than GFP-LRRK2 (*lane 7)*. All blots in the same row represent the same exposure on the same membrane. Preliminary experiments ensured that myc-LRRK2 and GFP-LRRK2 were expressed at similar levels (see *Experimental procedures*), which on these blots led to similar levels of GFP-LRRK2 and myc-LRRK2 observed in inputs. GFP-LRRK2 is not pulled down by myc resin in the absence of myc-LRRK2 (*lane 6)* and myc-LRRK2 is not pulled down by GFP antibody in the absence of GFP-LRRK2(*lane 8),* confirming specificity of IP.

(**D**) HMW LRRK2 contains LRRK2 dimer, assessed by heterologous co-IP. Myc-LRRK2 and GFP-LRRK2 were co-transfected into HEK293FT cells, and cell lysates were separated by glycerol velocity gradients into LMW and HMW pools of LRRK2. IP with high affinity myc resin co-IPed a substantially

greater amount of GFP-LRRK2, despite lower levels of myc- LRRK2 in the IP (lane 4). The small amount of co-IPed GFP-LRRK2 in the LMW fraction (lane 3) is likely a non-specific binding.

Figure 2. LRRK2 oligomerization state and activity in whole-cell lysates.

(**A**) Cell lysates containing endogenous or transfected LRRK2 were separated using glycerol gradients and LMW (L) and HMW (H) fractions were used for crosslinking using low concentrations of DSS. HMW LRRK2 is efficiently crosslinked into SDS-stable HMW complex, suggesting that glycerol gradients are not denaturing.

(**B**) Live MES cells transfected with LRRK2 were crosslinked with increasing concentrations of DSS, leading to a dose-dependent formation of SDS-stable HMW LRRK2 complexes.

(**C**) Crosslinking live MES cells (transfected with myc-LRRK2) with multiple reagents lead to formation of SDS-stable HMW LRRK2 complexes that migrate at similar molecular weights. DMSO (-) was the vehicle control. DSS (amines to amines, 11.4 Å), DST (amines to amines, 6.4 Å), SATP (amines to sulfhydryls, 4.1 Å), BMH (sulhydryls to sulfhydryls, 16.1 Å), BMOE (sulhydryls to sulfhydryls, 8.0 Å) were all dissolved to 20 mM in DMSO and used at the final concentration of 1 mM.

(**D**) Whole cell lysates from HEK293FT cells transfected with various myc-LRRK2 variants (WT, G2019S, R1441C or kinase-dead, KD) or an empty vector were used for myc IP and subsequent LRRK2 autophosphorylation assay. An autoradiograph of an SDS-PAGE gel separating the LRRK2 autophosphorylation reaction products shows increased incorporation of radioactive ^{32}P into G2019S LRRK2 compared to WT LRRK2, and lack of ^{32}P signal from the KD construct. The normalized LRRK2 kinase activity was quantified by measuring the intensity of ^{32}P-LRRK2 on the autoradiograph and normalizing to the amount of total LRRK2 as determined by Western blot. The normalized kinase activity for WT LRRK2 was arbitrarily set as 1. Both bands representing full-length LRRK2 were quantified, when present.

Figure 3. Subcellular localization of wild-type, mutant, and kinase-dead LRRK2.

(**A**) Cytosol and membrane fractions from MES cells transfected with wild-type (WT), R1441C or Y1699C LRRK2 do not show substantial differences in the localization of WT LRRK2 and PD-linked mutants. Cytosol and membrane fractions were volume normalized.

(**B**) WT-LRRK2 and KD-LRRK2 exhibit similar localization. Western blot analysis of LRRK2 from cytosol and membrane fractions of HEK293FT cells transfected with WT or KD LRRK2 show similar localization of both proteins, suggesting kinase activity is not a pre-requisite for membrane localization. All fractions were volume normalized and four times greater volume was loaded for membrane fraction to correct for the greater total levels found in the cytosol. Images were taken from the same western blot using cells transfected in parallel. The lower levels of KD LRRK2 found in both fractions (compared to WT) are likely due to the instability caused by the three mutations, which render it inactive.

Figure 4. Analysis of LRRK2 molecular weight by Blue-Native PAGE and size exclusion chromatography.

(**A**) LMW LRRK2 migrates on BN-PAGE as LRRK2 monomer, whereas migration of HMW LRRK2 corresponds to a dimer. Molecular weight standards were analyzed on the same gel and purchased either from GE Healthcare (GE) or Invitrogen (Inv).

(**B**) Addition of Triton-X100 substantially alters the estimated molecular weight of LRRK2 using size exclusion chromatography. Cytosol from cell lysates of HEK293FT cells transfected with myc-LRRK2 were separated using the Superdex 200 column in the absence of detergents or in the presence of increasing Triton-X100 concentrations (in both cell lysates and the mobile phase). The apparent estimated molecular weight of LRRK2 changes from ~ 1.3 MDa (maximum LRRK2 intensity without detergent) to a broad size of ~1.3 MDa - ~ 500 kDa upon addition of Triton-X100. The top panel represents the same blot shown in Figure 6. The major pool of eluted LRRK2 is shown in brackets and the apparent peaks distinguished by asterisks.

Figure 5. Kinase activity and GTP-binding of LRRK2 from cytosolic and membrane fractions.

(**A**) KD-LRRK2 does not exhibit kinase activity in membrane or cytosol fractions. Cytosol and membrane fractions from HEK293FT cells transfected with myc-LRRK2 (WT or KD) and untransfected cells (Untrans.) were used for myc IP and subsequent LRRK2 autophosphorylation assay. The kinase dead (KD) construct does not exhibit detectable kinase activity, suggesting that greater activity of membrane-associated LRRK2 is specific to the LRRK2 protein.

(**B**) WT-LRRK2 from membrane fraction phosphorylates a pseudosubstrate MBP (myelin basic protein) more efficiently than cytosolic LRRK2. Cytosol (Cyto) and membrane (Mem) extracts from HEK293FT transfected with WT LRRK2 or from untransfected cells (Untrans.) were IPed with myc resin and used for a kinase assay with MBP. Similar levels of LRRK2 were present in kinase reactions from cytosolic and membrane extracts. IP containing WT LRRK2 from the membrane fraction demonstrates higher kinase activity than that from cytosol.

(**C**) Endogenous membrane-associated LRRK2 binds GTP more efficiently than cytosolic LRRK2, despite lower LRRK2 levels in the input from the membrane fraction. Increasing amounts of protein were used for both fractions, below the saturating amount for the resin.

(**D**) Quantification of relative GTP binding of endogenous LRRK2 from human lymphoblasts (Mean ± SEM, n = 3).

(**E**) Cytosolic or membrane fractions containing transfected LRRK2 from dopaminergic MES cells were used for GTP binding. Increasing amounts of protein were used for both fractions, volume was kept constant for all samples. LRRK2 from the membrane fraction is pulled down more efficiently than that from cytosol, despite lower LRRK2 levels in the input from the membrane fraction.

Figure S1

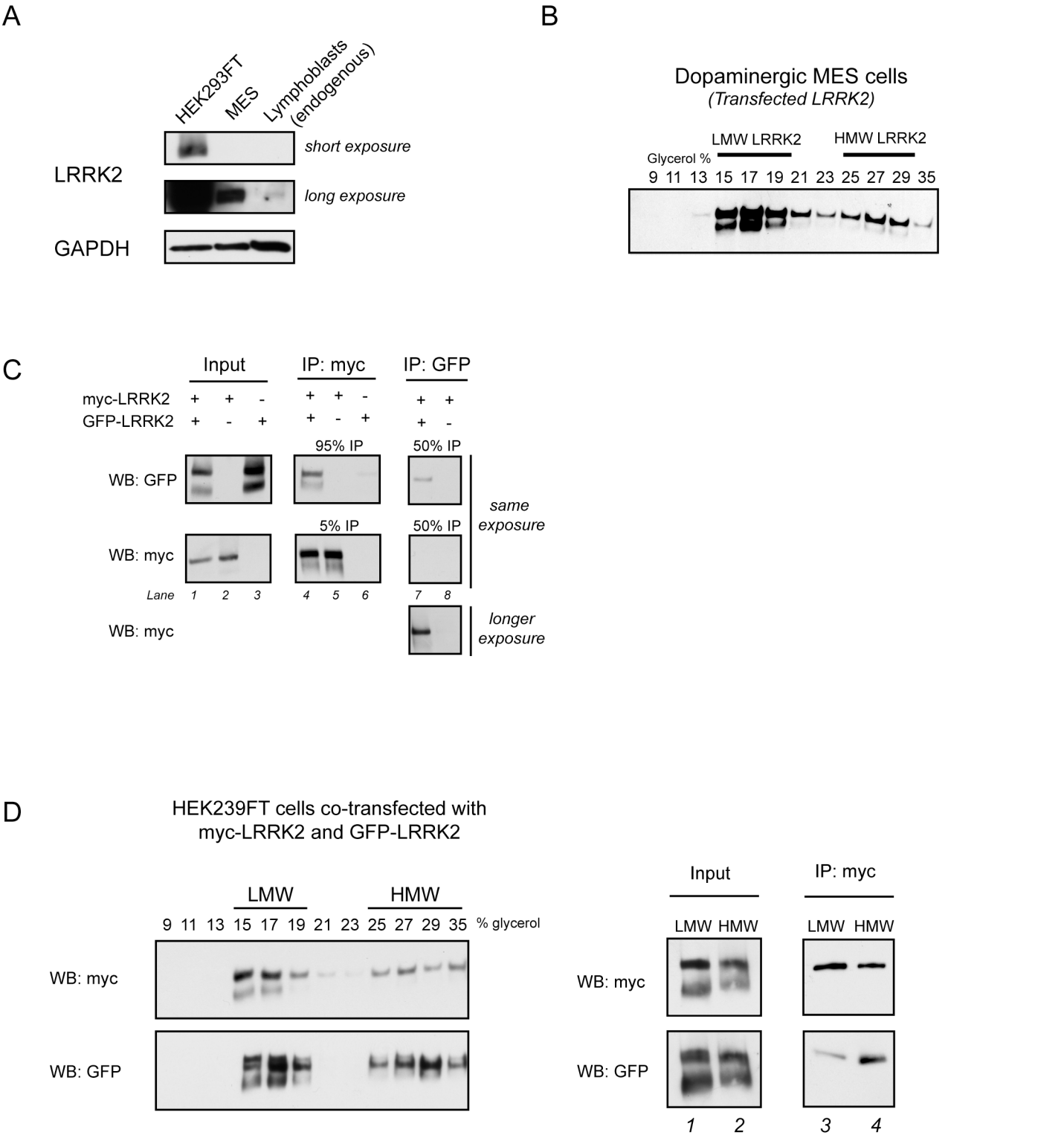
A
HEK293FT
MES
Lymphoblasts (endogenous)
LRRK2
short exposure
long exposure
GAPDH
B
Dopaminergic MES cells
(Transfected LRRK2)
LMW LRRK2
HMW LRRK2
Glycerol %
9 11 13 15 17 19 21 23 25 27 29 35
C
Input
IP: myc
IP: GFP
myc-LRRK2 + + - + + - + +
GFP-LRRK2 + - + + - + + -
95% IP
50% IP
WB: GFP
same exposure
5% IP
50% IP
WB: myc
Lane 1 2 3 4 5 6 7 8
WB: myc
longer exposure
D
HEK239FT cells co-transfected with myc-LRRK2 and GFP-LRRK2
LMW
HMW
9 11 13 15 17 19 21 23 25 27 29 35 % glycerol
WB: myc
WB: GFP
Input
IP: myc
LMW HMW
LMW HMW
WB: myc
WB: GFP
1 2 3 4

Figure S2

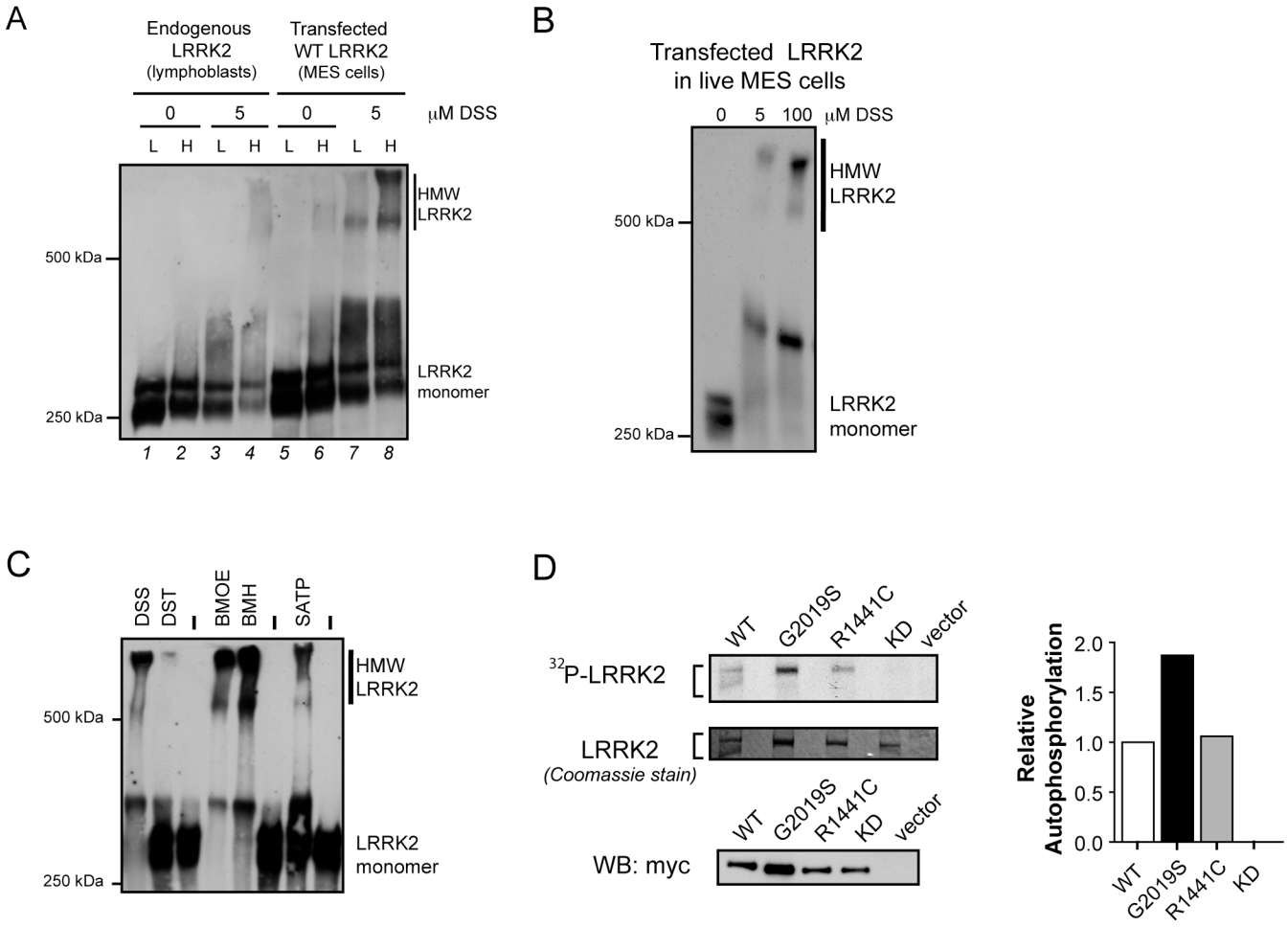

Figure S3

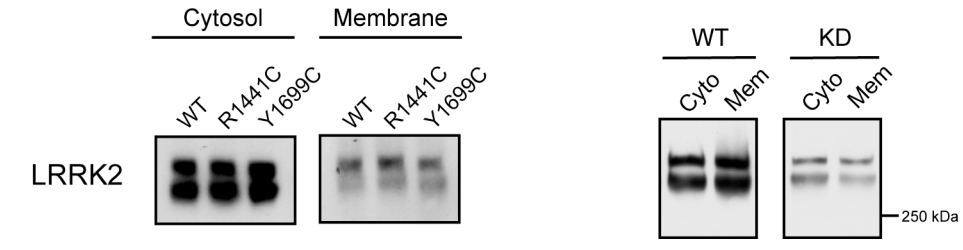

Figure S4

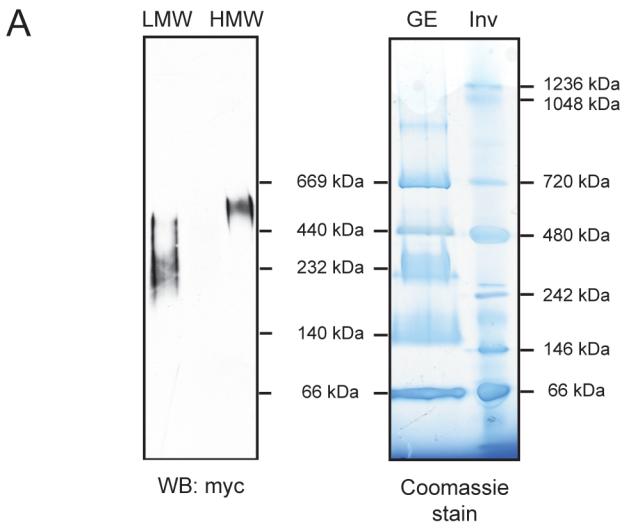
A
LMW
HMW
GE
Inv
1236 kDa
1048 kDa
669 kDa
720 kDa
440 kDa
480 kDa
232 kDa
242 kDa
140 kDa
146 kDa
66 kDa
66 kDa
WB: myc
Coomassie stain

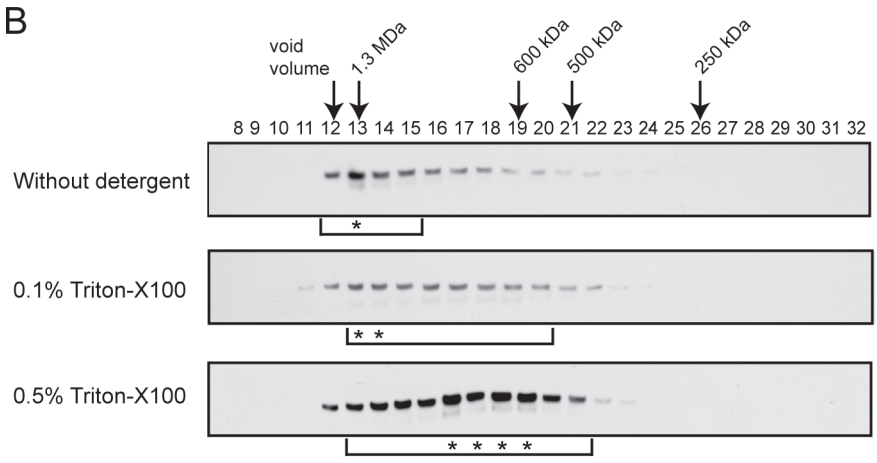
B
void volume
1.3 MDa
600 kDa
500 kDa
250 kDa
8 9 10 11 12 13 14 15 16 17 18 19 20 21 22 23 24 25 26 27 28 29 30 31 32
Without detergent
0.1% Triton-X100
0.5% Triton-X100

Figure S5

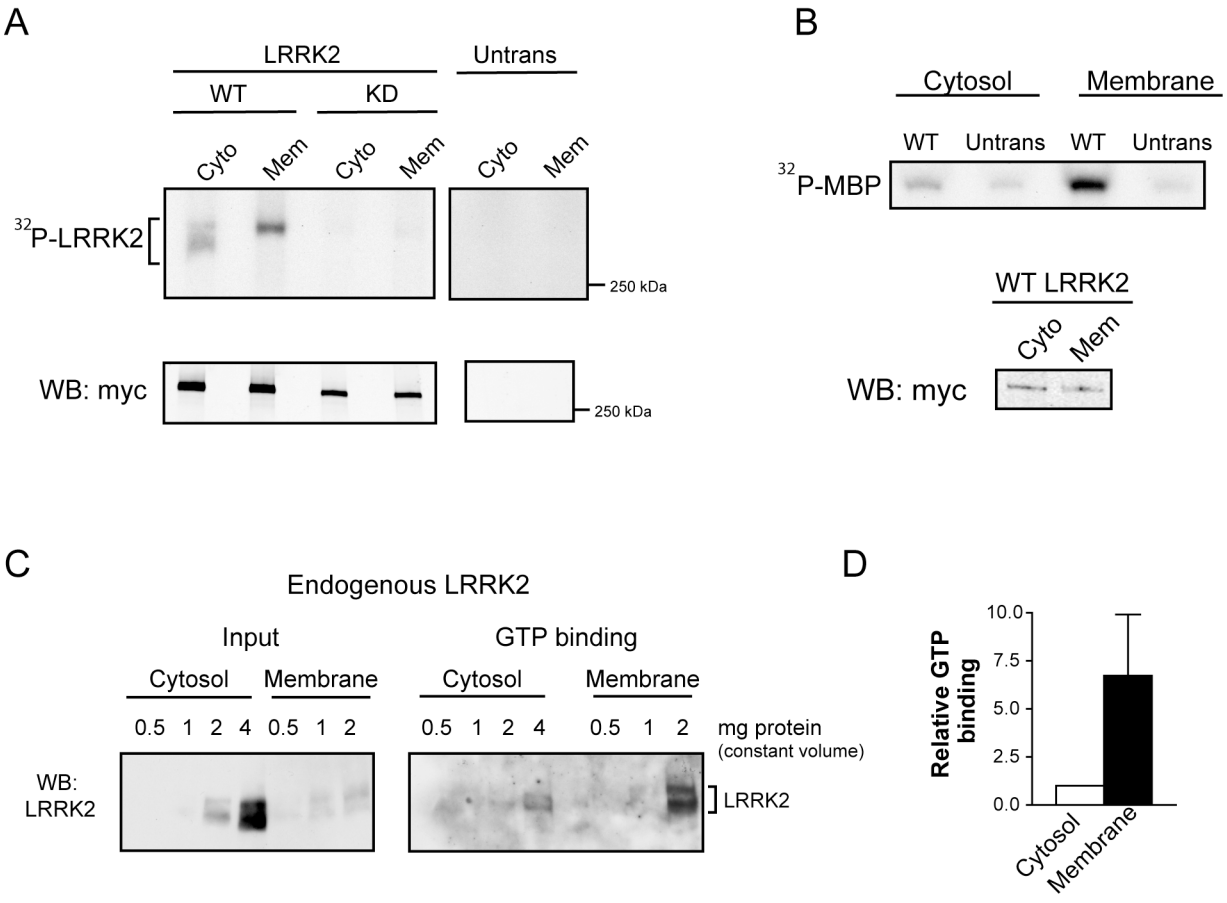
A
LRRK2
Untrans
WT
KD
Cyto
Mem
Cyto
Mem
Cyto
Mem
32P-LRRK2
250 kDa
WB: myc
250 kDa
B
Cytosol
Membrane
WT
Untrans
WT
Untrans
32P-MBP
WT LRRK2
Cyto
Mem
WB: myc
C
Endogenous LRRK2
Input
GTP binding
Cytosol
Membrane
Cytosol
Membrane
0.5 1 2 4 0.5 1 2
0.5 1 2 4 0.5 1 2
mg protein
(constant volume)
WB:
LRRK2
LRRK2
D
Relative GTP binding
10.0
7.5
5.0
2.5
0.0
Cytosol
Membrane
E
Transfected LRRK2 from dopaminergic MES cells
Input
GTP binding
Membrane
Cytosol
Membrane
Cytosol
0.5 1 2 4 0.5 1 2 4
0.5 1 2 4 0.5 1 2 4
mg protein
(constant volume)
WB:
myc